



Communication

A Nonlinear Magnetoelastic Energy Model and Its Application in Domain Wall Velocity Prediction

Li-Bo Wu^{1,2}, Yu-Feng Fan², Feng-Bo Sun³, Kai Yao^{1,*}  and Yue-Sheng Wang^{1,4,*} 

¹ Department of Mechanics, School of Civil Engineering, Beijing Jiaotong University, Beijing 100044, China; libo_wu@bjtu.edu.cn

² China Construction Second Bureau Installation Engineering Co., Ltd., Beijing 100176, China; yufengfan2020@163.com

³ China Construction Second Engineering Bureau Co., Ltd., Beijing 100160, China; sunfengbo@cscec.com

⁴ Department of Mechanics, School of Mechanical Engineering, Tianjin University, Tianjin 300350, China

* Correspondence: kaiy@bjtu.edu.cn (K.Y.); yswang@tju.edu.cn (Y.-S.W.)

Abstract: In this letter, we propose a nonlinear Magnetoelastic Energy (ME) with a material parameter related to electron interactions. An attenuating term is contained in the formula of the proposed nonlinear ME, which can predict the variation in the anisotropic magneto-crystalline constants induced by external stress more accurately than the classical linear ME. The domain wall velocity under stress and magnetic field can be predicted accurately based on the nonlinear ME. The proposed nonlinear ME model is concise and easy to use. It is important in sensor analysis and production, magneto-acoustic coupling motivation, magnetoelastic excitation, etc.

Keywords: nonlinear magnetoelastic energy; magneto-crystalline constants; domain wall velocity



Citation: Wu, L.-B.; Fan, Y.-F.; Sun, F.-B.; Yao, K.; Wang, Y.-S. A Nonlinear Magnetoelastic Energy Model and Its Application in Domain Wall Velocity Prediction. *Sensors* **2022**, *22*, 5371. <https://doi.org/10.3390/s22145371>

Academic Editor: Keat Ghee Ong

Received: 5 June 2022

Accepted: 15 July 2022

Published: 19 July 2022

Publisher's Note: MDPI stays neutral with regard to jurisdictional claims in published maps and institutional affiliations.



Copyright: © 2022 by the authors. Licensee MDPI, Basel, Switzerland. This article is an open access article distributed under the terms and conditions of the Creative Commons Attribution (CC BY) license (<https://creativecommons.org/licenses/by/4.0/>).

1. Introduction

Magnetoelastic Energy (ME) is essential in the guidance of magneto-acoustic coupling motivation [1–4], sensor production [5–8], and magnetoelastic excitation [9–11]. Classical Magnetoelastic Energy (ME) is a linear stress function that needs to be improved when predicting some specific aspects. However, many experiments indicate that the ME exhibits nonlinearity with increasing stress. The classical linear ME density can be expressed as $E_{me} = -3/2 \lambda_{s0} \sigma \cos \theta_{\sigma}$ [12], where λ_{s0} is the saturation magnetostriction coefficient without stress, σ is the stress, and θ_{σ} is the angle between the stress and magnetization. The Hamiltonian of the linear ME under displacement field $\mathbf{u}(\mathbf{r})$ is generally expressed as [2,13]:

$$\mathcal{H}_{me} = \frac{1}{s^2} \sum \int_V B_{\alpha\beta} s_{\alpha}(\mathbf{r}) s_{\beta}(\mathbf{r}) \varepsilon_{\alpha\beta}(\mathbf{r}) d\mathbf{r}, \quad (1)$$

where $\mathbf{r} = (x, y, z)$, $\alpha, \beta = x, y, z$; s is the saturation spin density; V is the volume; $\varepsilon_{\alpha\beta}(\mathbf{r})$ is the linear strain component which can be expressed as $\varepsilon_{\alpha\beta}(\mathbf{r}) = [\partial u_{\beta}(\mathbf{r})/\partial r_{\alpha} + \partial u_{\alpha}(\mathbf{r})/\partial r_{\beta}]/2$; $B_{\alpha\beta}$ is the magnetoelastic anisotropic constant; Ref. [2] and the Einstein summation convention is assumed.

Magnetization results from the electron's spin, which is related to the lattice parameters [1,12]. The magneto-elastic coupling effects are mainly relevant to the exchange field, spin-orbit coupling, etc. [12,13]. According to Refs. [14,15], the primary mechanism of the interactions between atoms (A and B) and electrons (a and b) are schematically plotted in Figure 1, where \mathbf{r}_{Aa} , \mathbf{r}_{Bb} , \mathbf{r}_{AB} , and \mathbf{r}_{ab} are position vectors. The red diamonds and green circles are the impacts of electrons a and b. The electrons' interactions are the primary influence factors of magnetization. It can be seen that the interactions of the electrons are related to the position vectors between electrons \mathbf{r}_{ab} . The expectation of electrons' distance

$|\overline{r_{ab}}|$ is also the function of Ψ . In addition, Ψ is the function of the nucleus position vector r_{AB} . Thus, $|\overline{r_{ab}}|$ can be expressed as:

$$|\overline{r_{ab}}| = \int \Psi_A^*(r_{AB}) \Psi_B^*(r_{AB}) |r_{ab}| \Psi_A(r_{AB}) \Psi_B(r_{AB}) dr, \quad (2)$$

where * means taking the conjugate.

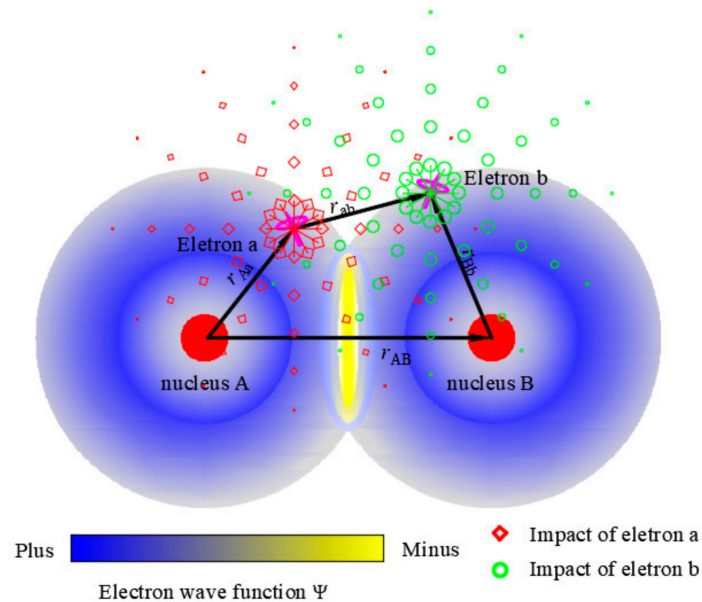


Figure 1. Primary mechanism of the interactions between atoms (A and B) and electrons (a and b).

The above is mainly the primary mechanism of the magnetoelastic effect [2,13]. ME is nonlinearly related to the nucleus distance. However, the classical linear ME includes only linear terms of Taylor's series [16–18]. The linear ME can describe the magnetoelastic behaviors under small deformation [1,2]. However, it becomes more ineffective in representing nonlinear behaviors with increasing deformation. Furthermore, if the higher-order nonlinear terms are taken to describe the nonlinear behaviors, the number of expansion coefficients to be determined increases rapidly, which is inconvenient to use. As far as we know, the constructive nonlinear ME is rarely reported, which is essential in the magnetoelastic behaviors under larger deformation.

In this letter, we construct a nonlinear ME with the material parameter to better and more conveniently describe nonlinear magnetoelastic behaviors. Then, the validity of the model was verified, and the model was applied in the prediction of the domain wall velocity under stress and a magnetic field, which is important in sensor production.

2. Model Construction

The derivation of the ME's density is mainly divided into three steps [16–18]. Firstly, the ME is expanded to the form of magneto-crystalline anisotropy energy in Taylor's series, and the first-order terms are taken as the ME approximately. Secondly, the expansion coefficients are solved under the equilibrium status without stress. Finally, the ME is obtained under the stress field.

In this letter, we construct a new function basis to expand ME by considering the following facts: (1) the new function basis should be complete and orthogonal; (2) the higher-order terms of ME should tend to be zero and be negligible; (3) material parameters should be included in the new function basis to describe different magnetoelasticity for various materials; (4) the increasing rate of ME is related to deformation [19,20]; and (5) ME increases more slowly with the increasing deformation [19,20].

Based on the above analysis, a series of new function bases with material parameters $[1, xe^{-|\vartheta x|}, x^2e^{-|\vartheta x|^2}, \dots, x^ne^{-|\vartheta x|^n}]$ are chosen instead of the polynomial function basis $[1, x, x^2, \dots, x^n]$, where $x = \varepsilon_{ij}$ is the strain component that is generally less than 1, and ϑ is the nonlinear material parameter related to the electron interactions. $e^{-|\vartheta\varepsilon_{ij}|}$ plays slight attenuating effects under larger strain (e.g., $\varepsilon > 10^{-2}$), and $\vartheta\varepsilon_{ij}$ is generally less than 10 by the nature of function $xe^{-|\vartheta x|}$. Thus, it is reasonable to assume that $\vartheta < 10^3$ in general. In addition, it is noted that $x^ne^{-|\vartheta x|^n}$ is closer to 0 as fast as x^n . Thus, the magneto-crystalline anisotropy energy density can be expressed as [12,13]:

$$E_k = E_k^0 + \sum_{i \geq j} \left(\frac{\partial E_k}{\partial (\varepsilon_{ij} e^{-|\vartheta\varepsilon_{ij}|})} \right) \varepsilon_{ij} e^{-|\vartheta\varepsilon_{ij}|} + \dots, \quad (3)$$

The first term (E_k^0) on the right-hand side of the above equation is the magneto-crystalline anisotropy energy density without stress. The remaining terms are the ME density (denoted by E_{me}), which can be viewed as the variation in the magneto-crystalline anisotropy energy density under stress. Generally, $\varepsilon_{ij} \ll 1$, and therefore, the second and higher-order terms are neglected. The expansion coefficients $\partial E_k / \partial (\varepsilon_{ij} e^{-|\vartheta\varepsilon_{ij}|})$ are related to the direction cosine ($\alpha_1, \alpha_2, \alpha_3$) of the magnetization vector. For the cubic crystal symmetry, the following equations are reasonable [13,16,18]:

$$\frac{\partial E_k}{\partial (\varepsilon_{ii} e^{-|\vartheta\varepsilon_{ii}|})} = B_1 \alpha_i^2, \quad i = 1, 2, 3, \quad (4)$$

$$\frac{\partial E_k}{\partial (\varepsilon_{ij} e^{-|\vartheta\varepsilon_{ij}|})} = B_2 \alpha_i \alpha_j, \quad i, j = 1, 2, 3 \text{ \& } i > j, \quad (5)$$

where B_1 and B_2 are the magnetoelastic coupling coefficients to be determined.

Therefore, the nonlinear ME density can be expressed as:

$$E_{me} = B_1 \sum_i^{1,2,3} \alpha_i^2 \varepsilon_{ii} e^{-|\vartheta\varepsilon_{ii}|} + B_2 \sum_{i>j}^{1,2,3} \alpha_i \alpha_j \varepsilon_{ij} e^{-|\vartheta\varepsilon_{ij}|}. \quad (6)$$

B_1 and B_2 can be solved based on the equilibrium conditions without external stress. Here, the free energy density (E) in the ferromagnetic crystal includes magneto-crystalline anisotropy energy density, ME density, and elastic energy density [16,18]. Only the magnetostrictive strain (denoted by ε_{ij}^λ) exists in ferromagnetic materials when no external stress is applied [12,13]. Thus, E can be expressed as:

$$\begin{aligned} E = & K_1 (\alpha_1^2 \alpha_2^2 + \alpha_2^2 \alpha_3^2 + \alpha_3^2 \alpha_1^2) \\ & + B_1 \sum_i^{1,2,3} \alpha_i^2 \varepsilon_{ii}^\lambda e^{-|\vartheta\varepsilon_{ii}^\lambda|} + B_2 \sum_{i>j}^{1,2,3} \alpha_i \alpha_j \varepsilon_{ij}^\lambda e^{-|\vartheta\varepsilon_{ij}^\lambda|} \\ & + \frac{1}{2} c_{11} \sum_i^{1,2,3} (\varepsilon_{ii}^\lambda)^2 + \frac{1}{2} c_{44} \sum_{i>j}^{1,2,3} (\varepsilon_{ij}^\lambda)^2 + c_{12} \sum_{i>j}^{1,2,3} \varepsilon_{ii}^\lambda \varepsilon_{jj}^\lambda, \end{aligned} \quad (7)$$

where c_{11} , c_{12} , and c_{44} are elastic constants, and K_1 is the magneto-crystalline anisotropy constant. The first term on the right-hand side of the above equation is the magneto-crystalline

anisotropy energy density E_k^0 . The sum of the last three items is the elastic energy density E_{el} for a cubic crystal. Then, B_1 and B_2 can be solved based on the equilibrium conditions:

$$\frac{\partial E}{\partial(\varepsilon_{ii})} = B_1 \alpha_i^2 e^{-|\vartheta \varepsilon_{ii}^\lambda|} (1 - |\vartheta \varepsilon_{ii}^\lambda|) + c_{11} \varepsilon_{ii}^\lambda + c_{12} (\varepsilon_{jj}^\lambda + \varepsilon_{kk}^\lambda) = 0, \quad (8)$$

$$i, j, k = 1, 2, 3 \text{ \& } k \neq j \neq i,$$

$$\frac{\partial E}{\partial(\varepsilon_{ij})} = B_2 \alpha_i \alpha_j e^{-|\vartheta \varepsilon_{ij}^\lambda|} (1 - |\vartheta \varepsilon_{ij}^\lambda|) + c_{44} \varepsilon_{ij}^\lambda = 0, \quad (9)$$

$$i, j = 1, 2, 3 \text{ \& } i > j.$$

Equations (8) and (9) are complicated to solve directly. However, the magnetostriction of non-giant magnetostrictive material is generally about 10^{-5} [21] and $\vartheta < 10^3$ based on the above analysis. Therefore, $\vartheta \varepsilon_{ij}^\lambda$ is near 0, and $e^{-|\vartheta \varepsilon_{ij}^\lambda|} \cong 1$. Thus, the term $B_1 \alpha_i^2 e^{-|\vartheta \varepsilon_{ij}^\lambda|} |\vartheta \varepsilon_{ij}^\lambda|$ in the above equations can be ignored. Then, Equations (8) and (9) can be simplified as:

$$B_1 \alpha_i^2 + c_{11} \varepsilon_{ii}^\lambda + c_{12} (\varepsilon_{jj}^\lambda + \varepsilon_{kk}^\lambda) = 0, \quad i, j, k = 1, 2, 3 \text{ \& } k \neq j \neq i, \quad (10)$$

$$B_2 \alpha_i \alpha_j + c_{44} \varepsilon_{ij}^\lambda = 0, \quad i, j = 1, 2, 3 \text{ \& } i > j. \quad (11)$$

The magnetostrictive strains ε_{ii}^λ and ε_{ij}^λ can be solved as:

$$\varepsilon_{ii}^\lambda = \frac{B_1 [c_{12} - \alpha_i^2 (c_{11} + 2c_{12})]}{(c_{11} - c_{12})(c_{11} + 2c_{12})}, \quad i = 1, 2, 3 \quad (12)$$

$$\varepsilon_{ij}^\lambda = -\frac{B_2 \alpha_i \alpha_j}{c_{44}}, \quad i \neq j \quad (13)$$

The micro-statistical method [22] is applied to construct the relationship between the coefficients $B_{1/2}$ and saturation magnetostriction λ_s , which can be measured by experiments. The following equations can be obtained for cubic crystals:

$$\lambda_s[100] = -\frac{B_1}{(c_{11} - c_{12})} \left(1 - \int_0^{2\pi} d\varphi \int_0^\pi \frac{1}{4\pi} \cos^2 \theta \sin \theta d\theta \right), \quad (14)$$

$$\lambda_s[111] = -\frac{B_2}{c_{44}} \left(\frac{1}{3} - \int_0^{2\pi} \frac{1}{4\pi} \sin \varphi \cos \varphi d\varphi \int_0^\pi \sin \theta d\theta \right), \quad (15)$$

where $\lambda_s[100]$ and $\lambda_s[111]$ are the saturation magnetostrictions without stress along [100] and [111], respectively. Then, B_1 and B_2 are solved as:

$$B_1 = -\frac{3}{2} \lambda_s[100] (c_{11} - c_{12}), \quad (16)$$

$$B_2 = -3 \lambda_s[111] c_{44}. \quad (17)$$

Considering a simple case, the external stress tensor can be expressed as $\sigma_{ij} = \sigma \gamma_{ij}$, where γ_{ij} is the direction cosine of the stress. The stress energy density $E_\sigma = \sum_{i \geq j} \sigma_{ij} \varepsilon_{ij}$ should be added in the free energy density E . Thus, the equilibrium conditions, Equations (8) and (9), change to:

$$\frac{\partial E}{\partial(\varepsilon_{ii})} = B_1 \alpha_i^2 e^{-|\vartheta \varepsilon_{ii}^\lambda|} (1 - |\vartheta \varepsilon_{ii}^\lambda|) + c_{11} \varepsilon_{ii}^\lambda + c_{12} (\varepsilon_{jj}^\lambda + \varepsilon_{kk}^\lambda) - \sigma \gamma_i^2 = 0, \quad (18)$$

$$i, j, k = 1, 2, 3 \text{ \& } k \neq j \neq i,$$

$$\frac{\partial E}{\partial(\varepsilon_{ij})} = B_2 \alpha_i \alpha_j e^{-|\vartheta \varepsilon_{ij}^\lambda|} (1 - |\vartheta \varepsilon_{ij}^\lambda|) + c_{44} \varepsilon_{ij}^\lambda - \sigma \gamma_i \gamma_j = 0, \quad (19)$$

$$i, j = 1, 2, 3 \text{ \& } i > j.$$

Generally, the magnetostriction is less than 10^{-5} . Thus, B_1 and B_2 are far less than elastic constants. $e^{-|\theta\epsilon_{ij}|}$ is less than 1, and $|\theta\epsilon_{ij}|e^{-|\theta\epsilon_{ij}|}$ is less than e^{-1} . As discussed above, the first terms on the right-hand side are far less than the second terms in Equations (18) and (19). Therefore, the first terms on the right-hand side can be ignored. The strain components are solved as:

$$\epsilon_{ii} = \frac{\sigma [c_{12} - \gamma_i^2 (c_{11} + 2c_{12})]}{(c_{11} - c_{12})(c_{11} + 2c_{12})}, \quad (20)$$

$$\epsilon_{ij} = \frac{\sigma \gamma_i \gamma_j}{c_{44}}, \quad i \neq j. \quad (21)$$

With the substitution of the magnetoelastic coupling coefficients (B_1 and B_2) and the direction-dependent terms of strain components into Equation (6), the nonlinear ME density, E_{me} , is obtained as:

$$E_{me} = -\frac{3}{2} \lambda_s [100] \sigma \sum_i^{1,2,3} \alpha_i^2 \gamma_i^2 e^{-|\frac{\theta \sigma \gamma_i^2}{(c_{11} - c_{12})}|} - 3 \lambda_s [111] \sigma \sum_{i>j}^{1,2,3} \alpha_i \alpha_j \gamma_i \gamma_j e^{-|\frac{\theta \sigma \gamma_i \gamma_j}{c_{44}}|}. \quad (22)$$

For an isotropic material, $\lambda_s [100] = \lambda_s [111] = \lambda_{s0}$, then Equation (22) can be written as:

$$E_{me} = \lambda_{s0} \sigma \left(-\frac{3}{2} \sum_i^{1,2,3} \alpha_i^2 \gamma_i^2 e^{-|\frac{\theta \sigma \gamma_i^2}{(c_{11} - c_{12})}|} - 3 \sum_{i>j}^{1,2,3} \alpha_i \alpha_j \gamma_i \gamma_j e^{-|\frac{\theta \sigma \gamma_i \gamma_j}{c_{44}}|} \right). \quad (23)$$

Under the uniaxial stress ($\gamma_i = 1, \gamma_j = \gamma_k = 0, i \neq j \neq k$), Equation (23) can be written as:

$$E_{me} = -\frac{3}{2} \lambda_{s0} \sigma \cos \theta_\sigma e^{-|\frac{\theta \sigma}{(c_{11} - c_{12})}|}, \quad (24)$$

where θ_σ is the angle between the stress and the magnetization.

The Hamiltonian of the nonlinear ME under displacement field $\mathbf{u}(\mathbf{r})$ can be applied in nanoscale fields. It can be expressed as:

$$\mathcal{H}_{me} = \frac{1}{s^2} \sum \int_V B_{\alpha\beta} e^{-|\theta \epsilon_{\alpha\beta}(\mathbf{r})|} s_\alpha(\mathbf{r}) s_\beta(\mathbf{r}) \epsilon_{\alpha\beta}(\mathbf{r}) d\mathbf{r}. \quad (25)$$

3. Model Verification

The variations in the magneto-crystalline anisotropy constant of CoFeB induced by ME with the stress applied along the x and y directions are given in Figure 2 [19]. The measurement was taken in a uniaxial in-plane anisotropy of the CoFeB/PVDF system. The magneto-crystalline anisotropy energy can be expressed by $E_k^0 = K_U (\alpha_1^2 + \alpha_2^2)$, where K_U is the magneto-crystalline anisotropy constant [23]. Considering both magnetization and stress along the x direction ($\alpha_1 = \gamma_1 = 1, \alpha_2 = \alpha_3 = \gamma_2 = \gamma_3 = 0$) or along the y direction ($\alpha_2 = \gamma_2 = 1, \alpha_1 = \alpha_3 = \gamma_1 = \gamma_3 = 0$), we have $E_k = E_k^0 + E_{me} = K_U + E_{me} / \cos \theta_\sigma$. Then, $E_{me} / \cos \theta_\sigma$ can be considered as the variation of K_U which is denoted as ΔK_U , i.e., $\Delta K_U = E_{me} / \cos \theta_\sigma$. Figure 2a presents the angular dependence of the normalized remanent magnetization (M_r / M_s), where M_r is the remanent magnetization, and M_s is the saturation magnetization. It shows a uniaxial anisotropy, and the easy axis is along the y direction. It should be reasonable to assume that the values of θ are different in different directions when the distribution of magnetic particles varies according to the physical meaning of θ . Therefore, the values of θ for CoFeB along with x and y are taken as $\theta_x = 45$ and $\theta_y = 52$, respectively. The film can be regarded as a two-dimensional material different from the three-dimensional material. Then, a reduction factor of one-half should be included approximately in the ME's density [24–27]. The saturation magnetostriction of CoFeB along both the x and y directions is taken as $\lambda_{s0} = 31$ ppm [20]. The relationship between the strain and stress of CoFeB is $\epsilon_{x/y} = \sigma_{x/y} (1 - \nu^2) / G$ [19,20], where G (~ 162 GPa [19,20]) is the elastic modulus, and ν (~ 0.3 [19,20]) is the Poisson's ratio of CoFeB. Thus, ΔK_U calculated

by the linear ME density and nonlinear ME density along the x and y directions, are given by:

$$\Delta K_{Ux/y} = -\frac{3}{4}\lambda_{s0}\sigma \quad (\text{Linear ME}) \quad (26)$$

$$\Delta K_{Ux/y} = -\frac{3}{4}\lambda_{s0}\sigma e^{-\left|\frac{\theta_{x/y}\sigma(1-\nu^2)}{G}\right|} \quad (\text{Nonlinear ME}) \quad (27)$$

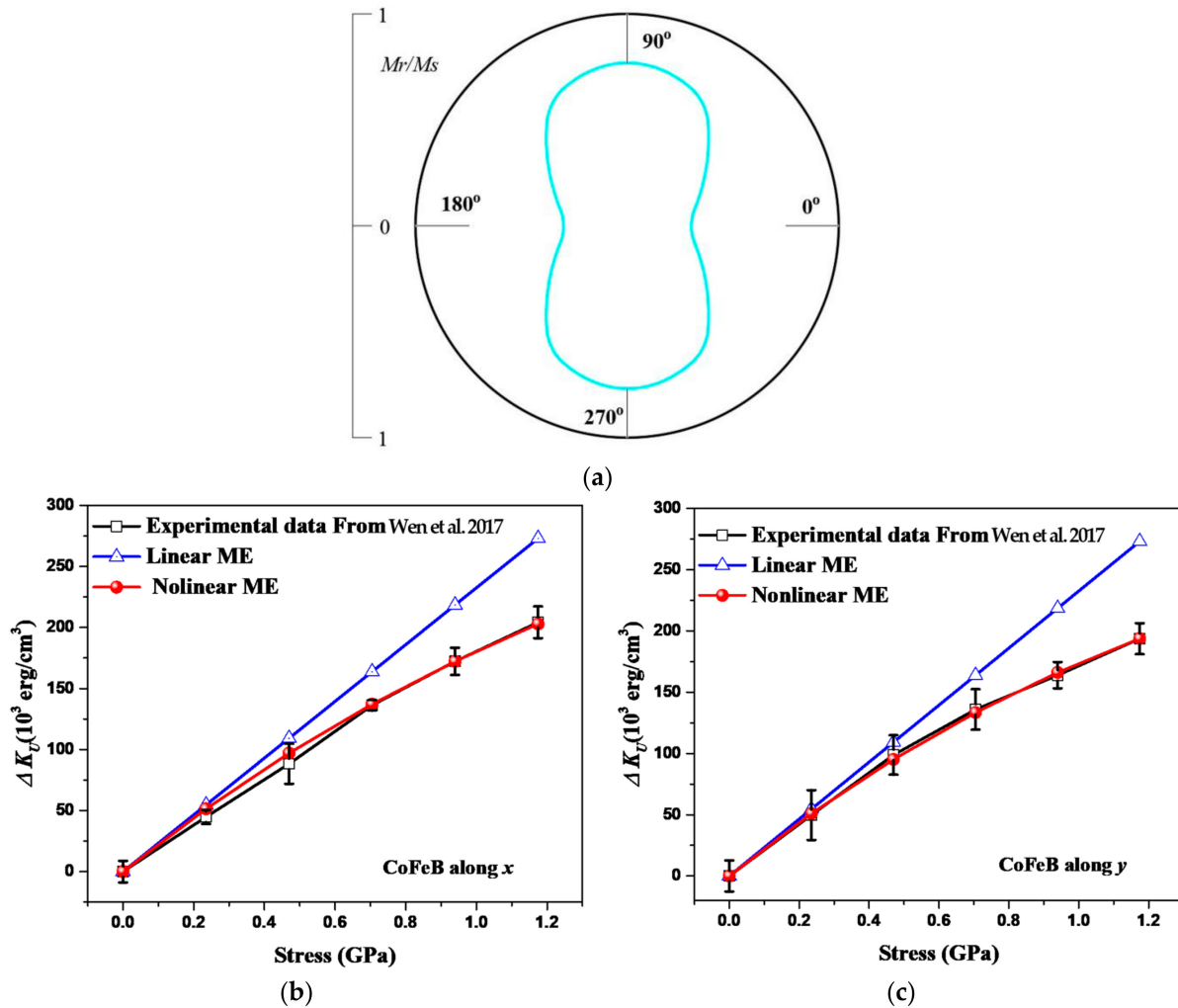


Figure 2. Comparison of the magnetic anisotropy constant variations in CoFeB by experiments [19] (Reproduced with permission from APPL. PHYS. LETT. 111(14), 142403 (2017). Copyright 2021 American Institute of Physics): (a) the definition of easy (x) and hard (y) magnetization directions, calculations by linear and proposed nonlinear ME (ME) along with x (b) and y (c) directions.

It is observed in Figure 2b,c that the measured ΔK_u along the x and y directions [19] (black lines with the square points) increases with the increasing stress. However, the rate of increase decreases, which is more obvious along the y direction than along the x direction. ΔK_u (blue lines with the triangular points) in Figure 2b,c predicted by the linear ME density exhibits linear growth along the x and y directions with the increasing stress. When the stress is small, the results predicted by the linear ME density are close to the experimental results in Ref. [19]. However, the predicted errors become larger with the increasing stress. In other words, the prediction for some specific aspects based on the linear ME needs to be improved. In addition, there was a problem predicting the anisotropy along the x and y directions based on the linear ME density. The ΔK_u predicted by the proposed nonlinear ME (red lines with the circular points) in Figure 2b,c exhibits nonlinear growth along the x

and y directions. It can predict the anisotropy as well. The predicted errors by nonlinear ME remain small with the increasing stress.

The ME can be regarded as the variation in magneto-crystalline energy under stress [12,13]. The magneto-crystalline constant is the magneto-crystalline energy density, with the angle's cosine being 1. It is demonstrated that the increasing trends of magneto-crystalline constants are nonlinear, see the experimental results in Figure 2b,c [19]. This phenomenon results from the interaction between magnetic particles that decay with the increasing distance between particles [12]. Compared with the linear ME density $E_{me}^{Linear} = -3/2\lambda_{s0}\sigma \cos \theta_\sigma$ [12], the proposed nonlinear ME density contains exponential terms and material parameters. It makes the nonlinear ME more capable of describing the decaying growth trend and the variations between materials of different magnetoelastic behaviors under larger deformation.

4. Model Application

The proposed nonlinear ME density can be used widely. According to the previous description, magnetic anisotropy is related to magneto-elastic energy. We predicted the effect of magnetic anisotropy induced by stress on the domain wall (DW) dynamics for Co-rich microwires based on the nonlinear ME density. The velocity of DW propagates along with the wire is known to be [28,29]:

$$v = S(H - H_0) \quad (28)$$

where H is the axial magnetic field, H_0 is the critical propagation field, and S is the DW mobility given by:

$$S = 2\mu_0 M_s / \beta \quad (29)$$

where β is the viscous damping coefficient [28,29]. Moreover, $\beta \approx M_s [K / (A/a)]^{1/2}$, where M_s is the saturation magnetization, A is the exchange stiffness constant, a is the distance between magnetic particles, and $K = K_0 + K_{me}$ is the magnetic anisotropy. Here, K_0 is the magnetic anisotropy without stress, and $K_{me} = -3/2 \lambda_{s0} \sigma e^{-|\theta_\sigma/G|}$ is the magnetic anisotropy induced by stress based on the proposed nonlinear ME.

As is known [28,29], the domain wall velocity is related to the interaction between magnetic particles, which decays with the increasing distance between particles. The viscous damping coefficient β decreases as the increasing stress within a certain range. The measured DW velocity on the magnetic field under stress is shown as the scatter points [28] in Figure 3. The calculated results based on the linear ME are shown as the lines in Figure 3a. It is shown that the domain wall velocity decreases with the increasing stress. It is obvious that β increases with the increasing stress. Then, S decreases, as can be seen from Equation (28). Thus, the calculated domain wall velocity based on the linear ME decreases with the increasing stress. It is different from the experimental results. The calculated results based on the proposed nonlinear ME are shown as the lines in Figure 3b. It is demonstrated that the DW velocity increases with the stress and the increasing magnetic field within the limited measurement range. The experimental and calculated results are in good agreement. The nonlinear magnetoelastic energy density can describe the nonlinear behaviors to a certain extent.

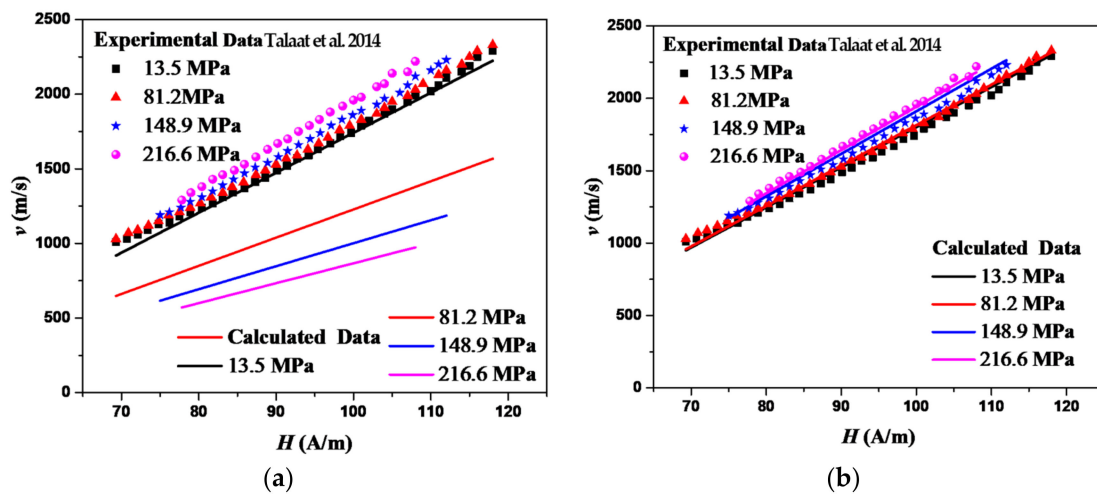


Figure 3. The predictions of DW velocity on magnetic field measured for $\text{Co}_{69.2}\text{Fe}_{4.1}\text{B}_{11.8}\text{Si}_{13.8}\text{C}_{1.1}$ microwires [28] under different tensile stresses based on the linear ME. (Reproduced with permission from IEEE Transactions on Magnetics 50, 1–4 (2014). Copyright 2022 IEEE) (a) and the proposed non-linear ME (b). The following parameters are used in the calculation: $K_0 = 8 \text{ J/m}^3$, $A/a = 1800 \text{ J/m}$, $\lambda_{s0} = 1 \times 10^{-7}$, $H_0 = 35 \text{ A/m}$, $\vartheta/G = 3.1 \times 10^{-8} \text{ Pa}^{-1}$, and $\nu = 0.3$.

5. Concluding Remarks

In this letter, the nonlinear magnetoelastic energy is constructed by expanding magnetoelastic energy based on magneto-crystalline anisotropy energy by applying a new function basis with material parameters. It can describe the different materials' nonlinear magnetoelastic behaviors. The coefficients are determined by saturation magnetostriction, which can be measured in experiments. The proposed nonlinear magnetoelastic energy can better predict the experimental results of the magneto-crystalline anisotropy constant variation and anisotropy under the stress field than the classical linear magnetoelastic energy. Based on the nonlinear magnetoelastic energy, the domain wall velocity under stress and the magnetic field can be predicted accurately. The Hamiltonian of the nonlinear ME applied in nanoscale fields is obtained. It has promising applications in a wider range of fields, e.g., sensor production, magneto-acoustic coupling motivation, magnetic memory method testing, magnetoelastic excitation, etc.

Author Contributions: Conceptualization, Y.-S.W., K.Y. and L.-B.W.; methodology, Y.-S.W., K.Y., L.-B.W. and Y.-F.F.; formal analysis, L.-B.W., K.Y., F.-B.S. and Y.-F.F.; investigation, Y.-F.F. and F.-B.S.; data curation, L.-B.W.; writing—original draft preparation, L.-B.W., Y.-F.F. and F.-B.S.; writing—review and editing, Y.-S.W. and K.Y.; supervision, Y.-S.W. and K.Y.; project administration, K.Y.; funding acquisition, K.Y. and L.-B.W. All authors have read and agreed to the published version of the manuscript.

Funding: This work is financially supported by the National Natural Science Foundation of China (No. 11872104), China State Construction Engineering Corporation (No. CSCEC-2021-Q-55) and Fundamental Research Funds for the Central Universities (No. 2019JBM82).

Institutional Review Board Statement: Not applicable.

Informed Consent Statement: Not applicable.

Data Availability Statement: Not applicable.

Conflicts of Interest: The authors declare that they have no known competing financial interests or personal relationships that could have appeared to influence the work reported in this paper.

References

1. Cornelissen, L.J.; Liu, J.; Duine, R.A.; Youssef, J.B.; van Wees, B.J. Long-distance transport of magnon spin information in a magnetic insulator at room temperature. *Nat. Phys.* **2015**, *11*, 1022. [\[CrossRef\]](#)
2. Zhang, S.; Shi, Y.; Gao, Y. Tunability of band structures in a two-dimensional magnetostrictive phononic crystal plate with stress and magnetic loadings. *Phys. Lett. A* **2017**, *381*, 1055–1066. [\[CrossRef\]](#)
3. Arena, D.A.; Vescovo, E.; Kao, C.C.; Guan, Y.; Bailey, W.E. Weakly coupled motion of individual layers in ferromagnetic resonance. *Phys. Rev. B* **2006**, *74*, 064409. [\[CrossRef\]](#)
4. Dai, M.; Chen, X.; Sun, T.; Yu, L.; Chen, M.; Lin, H.; Chen, S. A 2D Magneto-Acousto-Electrical Tomography method to detect conductivity variation using multifocus image method. *Sensors* **2018**, *18*, 2373. [\[CrossRef\]](#)
5. Saiz, P.G.; Porro, J.M.; Lasheras, A.; Luis, R.; Lopes, A.C. Influence of the magnetic domain structure in the mass sensitivity of magnetoelastic sensors with different geometries. *J. Alloys Compd.* **2021**, *863*, 158555. [\[CrossRef\]](#)
6. Grenda, P.; Kutyla, M.; Nowicki, M.; Charubin, T. Bendductor—Transformer Steel Magnetomechanical Force Sensor. *Sensors* **2021**, *21*, 8250. [\[CrossRef\]](#)
7. Meydan, T.; Oduncu, H. Enhancement of magnetostrictive properties of amorphous ribbons for a biomedical application. *Sens. Actuators A Phys.* **1997**, *59*, 192–196. [\[CrossRef\]](#)
8. Samourganidis, G.; Kouzoudis, D. Magnetoelastic Ribbons as Vibration Sensors for Real-Time Health Monitoring of Rotating Metal Beams. *Sensors* **2021**, *21*, 8122. [\[CrossRef\]](#)
9. Mansourian, S.; Bakhshayeshi, A. Giant magneto-impedance variation in amorphous CoFeSiB ribbons as a function of tensile stress and frequency. *Phys. Lett. A* **2020**, *384*, 126657. [\[CrossRef\]](#)
10. Sisniega, B.; Sagasti Sedano, A.; Gutiérrez, J.; García-Arribas, A. Real time monitoring of calcium oxalate precipitation reaction by using corrosion resistant magnetoelastic resonance sensors. *Sensors* **2020**, *20*, 2802. [\[CrossRef\]](#)
11. Strecka, J.; Rojas, O.; Souza, S.D. Absence of a spontaneous long-range order in a mixed spin-(1/2, 3/2) Ising model on a decorated square lattice due to anomalous spin frustration driven by a magnetoelastic coupling. *Phys. Lett. A* **2019**, *383*, 2451–2455. [\[CrossRef\]](#)
12. Chikazumi, S.; Graham, C.D. *Physics of Ferromagnetism 2e*; Oxford University Press on Demand: Oxford, UK, 2009.
13. Gurevich, A.G.; Melkov, G.A. *Magnetization Oscillations and Waves*; CRC Press: Boca Raton, FL, USA, 1996.
14. Itatani, J.; Levesque, J.; Zeidler, D.; Niikura, H.; Pépin, H.; Kieffer, J.C.; Villeneuve, D.M. Tomographic imaging of molecular orbitals. *Nature* **2004**, *432*, 867–871. [\[CrossRef\]](#) [\[PubMed\]](#)
15. Rana, A.; Zhang, J.; Pham, M.; Yuan, A.; Lo, Y.H.; Jiang, H.; Miao, J. Potential of attosecond coherent diffractive imaging. *Phys. Rev. Lett.* **2020**, *125*, 086101. [\[CrossRef\]](#) [\[PubMed\]](#)
16. Liu, S.H. New magnetoelastic interaction. *Phys. Rev. Lett.* **1972**, *29*, 793. [\[CrossRef\]](#)
17. Pesquera, D.; Skumryev, V.; Sanchez, F.; Herranz, G.; Fontcuberta, J. Magnetoelastic coupling in $\text{La}_2/3\text{Sr}_1/3\text{MnO}_3$ thin films on SrTiO_3 . *Phys. Rev. B* **2011**, *84*, 184412. [\[CrossRef\]](#)
18. Rinaldi, S.; Turilli, G. Theory of linear magnetoelastic effects. *Phys. Rev. B* **1985**, *31*, 3051. [\[CrossRef\]](#)
19. Wen, X.; Wang, B.; Sheng, P.; Hu, S.; Yang, H.; Pei, K.; Li, R.W. Determination of stress-coefficient of magnetoelastic anisotropy in flexible amorphous CoFeB film by anisotropic magnetoresistance. *Appl. Phys. Lett.* **2017**, *111*, 142403. [\[CrossRef\]](#)
20. Wang, D.; Nordman, C.; Qian, Z.; Daughton, J.M.; Myers, J. Magnetostriction effect of amorphous CoFeB thin films and application in spin-dependent tunnel junctions. *J. Appl. Phys.* **2005**, *97*, 10C906. [\[CrossRef\]](#)
21. Hathaway, K.B.; Clark, A.E. Magnetostrictive materials. *MRS Bull.* **1993**, *18*, 34–41. [\[CrossRef\]](#)
22. Wu, L.B.; Yao, K.; Zhao, B.X.; Wang, Y.S. A micro-statistical constructive model for magnetization and magnetostriction under applied stress and magnetic fields. *Appl. Phys. Lett.* **2019**, *115*, 162406. [\[CrossRef\]](#)
23. Asti, G.; Bolzoni, F. Theory of first order magnetization processes: Uniaxial anisotropy. *J. Magn. Magn. Mater.* **1980**, *20*, 29–43. [\[CrossRef\]](#)
24. Song, O. Magnetoelastic Coupling in Thin Films. Ph.D. Thesis, Massachusetts Institute of Technology, Cambridge, MA, USA, 1994.
25. Tian, Z.; Sander, D.; Jürgen, K. Nonlinear magnetoelastic coupling of epitaxial layers of Fe, Co, and Ni on Ir(100). *Phys. Rev. B* **2009**, *79*, 024432. [\[CrossRef\]](#)
26. Yi, M.; Xu, B.X.; Shen, Z. 180 magnetization switching in nanocylinders by a mechanical strain. *Extrem. Mech. Lett.* **2015**, *3*, 66–71. [\[CrossRef\]](#)
27. Tang, Z.H.; Jiang, Z.S.; Chen, T.; Lei, D.J.; Yan, W.Y.; Qiu, F.; Huang, J.-Q.; Deng, H.-M.; Yao, M. Simultaneous microwave photonic and phononic band gaps in piezoelectric–piezomagnetic superlattices with three types of domains in a unit cell. *Phys. Lett. A* **2016**, *380*, 1757–1762. [\[CrossRef\]](#)
28. Talaat, A.; Blanco, J.M.; Ipatov, M.; Zhukova, V.; Zhukov, A.P. Domain wall propagation in Co-based glass-coated microwires: Effect of stress annealing and tensile applied stresses. *IEEE Trans. Magn.* **2014**, *50*, 1–4. [\[CrossRef\]](#)
29. Moubah, R.; Magnus, F.; Kapaklis, V.; Hjärvansson, B.; Andersson, G. Anisotropic Magnetostriction and Domain Wall Motion in $\text{Sm}_{10}\text{Co}_{90}$ Amorphous Films. *Appl. Phys. Express* **2013**, *6*, 053004. [\[CrossRef\]](#)